ARCHIVES
of
FOUNDRY ENGINEERING

10.24425/afe.2026.157997

Published quarterly as the organ of the Foundry Commission of the Polish Academy of Sciences

ISSN (2299-2944)
Volume 2026
Issue 2/2026

118 – 127

14/2

Optimization of Rotary Degassing Parameters to Improve Melt Cleanliness and Mechanical Properties in A356 Aluminum Alloy

U. Kutsal [a, *], M. Çolak [b], Y. Sağnak [a], S. Bardakcı [a], G. Ammas [a], G. Sarper [a]
[a] Cevher Jant Sanayii A.Ş. Turkey
[b] Bayburt University, Turkey
* Corresponding author: E-mail address: umit.kutsal@cevher.com

Received 05.11.2025; accepted in revised form 23.02.2026; available online 14.07.2026

Abstract

Melt cleanliness is a critical factor that directly affects the quality of aluminum castings and becomes even more significant in recycling-oriented production, where high scrap utilization is inevitable. Increasing the proportion of scrap intensifies the risk of oxide films, inclusions, and gas porosity in the molten metal; therefore, efficient refining techniques are essential. In this study, the effects of rotary degassing parameters—including rotor speed, rotation time, and gas flow rate—on melt cleanliness of A356 aluminum alloy were systematically investigated. Experimental melts containing 20% primary and 80% scrap aluminum were treated under various degassing conditions using a commercial flux cleaning flux. Characterization was performed through the Reduced Pressure Test (RPT), bifilm index analysis, fluidity measurements, microstructural examinations, and mechanical testing (tensile test and Brinell hardness measurement). The results demonstrated that increasing the rotor speed from 200 rpm to 500 rpm significantly reduced both the density and bifilm indices, indicating a notable improvement in melt cleanliness. Furthermore, higher gas flow rate (10 L/min) and longer rotation time (10 min) provided additional but secondary improvements. Consequently, the optimization of rotary degassing parameters enhanced not only melt quality but also tensile strength and ductility. These findings offer practical insights for optimizing process control in recycling-based aluminum foundries.

Keywords: A356 aluminum alloy, Rotary degassing, Melt cleanliness, Bifilm index, Recycling, Mechanical properties

1. Introduction

Aluminum alloys, owing to their low density, superior mechanical and structural properties, cost-effectiveness, and excellent corrosion and oxidation resistance, represent the second most widely used metallic material group after ferrous alloys. Their ability to be processed through various manufacturing techniques further enhances their versatility. These advantageous characteristics have led to the widespread use of aluminum alloys across numerous industrial sectors. In particular, the demand for aluminum alloys in the automotive industry has been steadily increasing due to the global trend toward lightweight and energy-efficient vehicle design [1–4]. Aluminum production can be achieved through two main routes: primary production from ore and secondary production through recycling of scrap. In primary production, bauxite ore is refined via the Bayer process to obtain alumina, which is then reduced electrolytically to produce pure aluminum. This method is highly energy intensive and requires significant infrastructure investment [5]. In contrast, secondary aluminum production offers substantial energy savings—up to 95% compared to primary production—and has become indispensable due to its lower raw material costs and reduced environmental impact [6]. However, the extensive use of secondary aluminum introduces certain challenges, such as the presence of impurities, inclusions, detrimental intermetallic compounds, and oxide films. These defects often originate from natural impurities, intentionally added alloying elements, or contaminants carried from scrap sources [7]. Such inclusions and oxides increase the likelihood of porosity and film formation, consequently deteriorating mechanical properties, fluidity, feeding behavior, and castability of aluminum alloys [8]. Therefore, in recycling-based production, the most critical issue is optimizing melt quality and implementing additional refining treatments during casting. Poor melt cleanliness not only increases the scrap rate but also leads to reduced fluidity, micro-porosity formation, cracking, and deterioration in mechanical performance [9–11]. To address these issues, numerous melt treatment techniques—ranging from inert gas purging to flux and tablet-based refiners—have been developed. Among these, commonly adopted refining methods include flux treatment, gas injection using nitrogen lances, rotary degassing, re-melting degassing, electromagnetic and ultrasonic degassing, and vacuum degassing [12].

Foundries employ different melt-cleaning techniques depending on their production capacity and process design. To assess the effectiveness of these refining operations, several testing methods have been developed. Among them, the Reduced Pressure Test (RPT) and K-mold technique are the most widely used due to their low investment cost, rapid results, and operational simplicity. The RPT is based on the principle of solidifying molten aluminum under vacuum conditions to promote the formation of visible gas porosity. In this method, the pressure inside the test chamber is reduced to approximately 80 mbar. About 100 g of molten metal is poured into a steel crucible and allowed to solidify under vacuum. For comparison, an identical sample is also solidified under atmospheric conditions. The two samples are then examined by visual inspection, density measurements, or image analysis after standard metallographic preparation. A lower number of pores indicates a cleaner melt with reduced hydrogen and oxide content [13–16]. The K-mold test, on the other hand, is a fracture-based technique designed to evaluate the macroscopic cleanliness of molten aluminum prior to casting. Compared with other melt-quality assessment methods, it offers several advantages such as low cost, simple sampling, rapid evaluation, and high sensitivity to inclusions and oxide films. After casting, the specimens are removed from the mold, fractured at the notched section, and the fracture surfaces are examined macroscopically. Due to rapid solidification in thin cross-sections, inclusions and oxide films become visible on the fracture surfaces, allowing a qualitative assessment of melt cleanliness [16–18].

Considering the growing importance of recycling-based production and the necessity of maintaining high melt cleanliness during the reuse of scrap aluminum, this topic holds significant industrial relevance. Therefore, in the present study, the effects of rotary degassing process parameters—namely rotor speed, rotation time, and gas flow rate—on melt cleanliness in A356 aluminum alloy containing 20% primary and 80% scrap material were systematically investigated. During the experiments, a commercially cleaning flux was used in combination with various degassing parameter settings. The resulting cast samples were comprehensively characterized using multiple complementary techniques, including the Reduced Pressure Test (RPT), bifilm index analysis, fluidity testing, microstructural observations, and tensile testing. This multifaceted approach enabled a detailed evaluation of how rotary degassing parameters influence both melt quality and mechanical performance.

2. Experimental Procedure

In this study, an A356 aluminum casting alloy containing 20% primary and 80% scrap material was used. To evaluate melt cleanliness, the effects of rotary degassing parameters—rotor speed, rotation time, and gas flow rate—were systematically investigated using a conventional cleaning flux. The experimental matrix was designed to include two levels for each parameter: rotor speeds of 200 rpm and 500 rpm, rotation times of 5 min and 10 min, and gas flow rates of 5 L/min and 10 L/min. These combinations were selected to determine the optimal degassing conditions for improved melt cleanliness and casting quality. The experimental parameters are summarized in Table 1.

Table 1.
Experimental Parameter

	Alloy	Addition of flux	Rotor Speed (rpm)	Rotation Time (min)	Gas Flow Rate (L/min)
1	A356 (20% primary + 80% secondary)	Yes	200	5	5
2	A356 (20% primary + 80% secondary)	Yes	200	5	10
3	A356 (20% primary + 80% secondary)	Yes	200	10	5
4	A356 (20% primary + 80% secondary)	Yes	200	10	10
5	A356 (20% primary + 80% secondary)	Yes	500	5	5
6	A356 (20% primary + 80% secondary)	Yes	500	5	10
7	A356 (20% primary + 80% secondary)	Yes	500	10	5
8	A356 (20% primary + 80% secondary)	Yes	500	10	10

The rotary degassing experiments were conducted using a side-perforated rotor head design, which was kept constant throughout all trials to ensure experimental consistency. A commercial cleaning flux was added to the melt at a ratio of 0.1 wt% prior to degassing. For each alloy composition, three casting repetitions were performed to ensure repeatability of the results. The pouring temperature was maintained at 700 °C for all experiments. The permanent molds were coated with Dycote 34 to ensure consistent surface conditions and heat transfer during casting. Mold coating was kept constant for all experiments to eliminate its influence on fluidity and melt quality. The permanent molds were coated with Dycote 34 mold coating and preheated to 250 °C before casting. During the trials, the molten alloy was poured into various mold types, including mechanical test mold, step mold, eight-channel fluidity mold, and Reduced Pressure Test (RPT) mold.

The melting of the alloy was carried out in an electric resistance furnace with a power of 10 kW and a capacity of 8 kg, using a silicon carbide (SiC) crucible. The alloy charge was prepared according to the predefined experimental parameters and loaded into the crucible. After melting, the molten metal was heated to the pouring temperature of 700 °C, and casting was performed directly from the crucible into the molds at 700 °C liquid metal temperature. Pouring time was 4 seconds for tensile test molds, 3 seconds for fluidity test molds and 1 seconds for reduced pressure test molds. After solidification was completed, the cast samples were removed from the molds and prepared for subsequent examinations. In the present study, melt quality evaluation was performed using RPT and an eight-channel fluidity mold; K-mold and spiral fluidity tests were not employed. Figure 1 shows a representative example photographic view of the samples after removal from the molds.

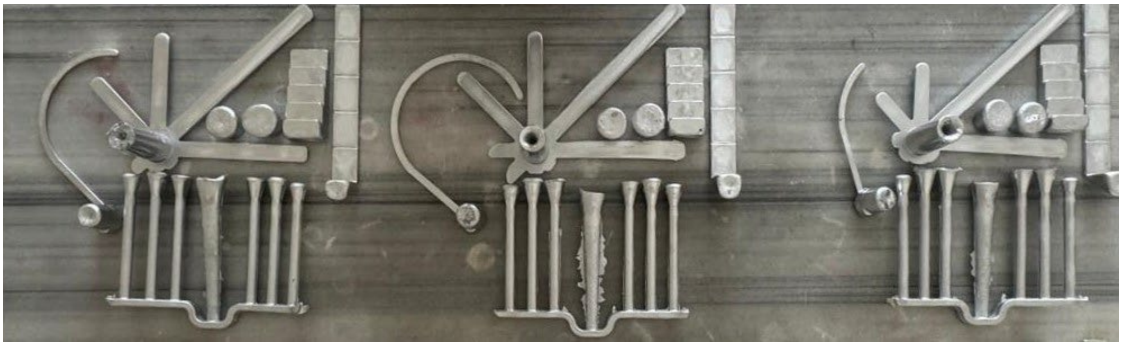

Fig. 1. Photographic view of the cast samples after removal from the molds

During the melt-cleaning stage, a rotary degassing process was applied. In this method, a graphite shaft and impeller system were immersed into the molten metal and rotated at the specified rotor speeds. Inert nitrogen gas (N_2) was introduced through the shaft while it was rotating, generating fine bubbles that dispersed throughout the melt due to the vortex created by rotation. The combined effect of gas flow and rotation promoted the removal of hydrogen gas, inclusions, and oxide films, which were carried to the surface of the melt.

After solidification and cooling, the molds were opened to obtain samples from the RPT, eight-channel fluidity, and mechanical test molds. The melt flow length for each section of the fluidity mold was measured to assess the flow behavior of the alloy. Melt flow length is influenced by several interrelated parameters, including liquid metal temperature, mold temperature, pouring rate, and gating conditions, all of which affect heat transfer and flow stability during mold filling [8, 9]. In the present study, liquid metal temperature, mold preheating temperature, and pouring conditions were kept constant to isolate the effect of melt cleanliness on fluidity behavior. To minimize these variations, a fluidity index was developed. The index was calculated by dividing the melt flow length in each channel by its corresponding section thickness and summing all results [8]. Thus, the flow behavior of the alloy is presented in terms of the fluidity index, providing a more standardized evaluation.

The samples obtained from the RPT molds were evaluated for density using the Archimedes' principle. Both atmospheric and vacuum-solidified specimens were measured in air and water, and the corresponding density index values were calculated. To observe internal porosity, each RPT sample was sectioned vertically at the center. The cut surfaces were then ground sequentially with 100-mesh and 400-mesh abrasive papers. Finally, the polished surfaces were digitally scanned to obtain high-resolution images for further pore analysis. For the determination of mechanical properties, tensile tests were conducted. The specimens obtained from the mechanical test mold were machined on a CNC lathe to the standard tensile geometry after removing the gating system. Tensile tests were performed on a Zwick Z100 testing machine with a maximum load capacity of 100 kN, following the EN ISO 6892-1 standard. From these tests, the yield strength, ultimate tensile strength, and elongation (%) values were determined for each casting condition.

3. Results and Discussion

3.1. Determination of Chemical Composition

The chemical composition of the cast samples obtained from the experiments was analyzed using an optical emission spectrometer (OES) to verify alloy conformity. The analyses were performed with an ARL-brand optical spectrometer in accordance with the EN 1706 standard. The chemical composition results of the A356 aluminum alloy are presented in Table 2.

Table 2.
Chemical composition results of the casting experiments (wt.%)

	Si	Fe	Cu	Mn	Mg	Ti	Cr	Ni	Sr	Al
Exp.1	7.15	0.18	0.00076	0.010	0.238	0.12	0.0012	0.0044	0.00383	92.2639
Exp.2	6.92	0.18	0.00078	0.0044	0.240	0.12	0.0013	0.0045	0.00013	92.4988
Exp.3	7.09	0.18	0.00072	0.0034	0.235	0.12	0.0014	0.0042	0.00599	92.3325
Exp.4	6.94	0.18	0.00077	0.0029	0.239	0.12	0.0013	0.0045	0.00505	92.4757
Exp.5	7.32	0.18	0.00074	0.0028	0.232	0.12	0.0014	0.0043	0.00390	92.1109
Exp.6	7.10	0.18	0.00073	0.0028	0.245	0.12	0.0013	0.0042	0.00566	92.3186
Exp.7	6.84	0.18	0.00073	0.0027	0.234	0.12	0.0012	0.0042	0.00702	92.5858
Exp.8	6.99	0.18	0.00079	0.0031	0.238	0.12	0.0016	0.0046	0.00388	92.4179

By examining the chemical compositions presented in Table 2, it was observed that all experimental alloys conformed to the A356 standard composition range. After determining the proportions of primary and scrap materials, the alloys were prepared to maintain a constant Fe content. The Fe concentration in all experiments was found to be between 0.175% and 0.22%, which is within the acceptable limits defined for A356 aluminum alloys.

3.2. Analysis of Melt Quality

In this study, casting experiments were performed under different rotary degassing conditions, including variations in rotor speed, gas flow rate, and rotation time. The average density index values obtained from the RPT samples were calculated and analyzed to evaluate melt cleanliness. The comparative results are illustrated in Figure 2.

$$\text{Density Index} = \frac{d_{atm} - d_{vacuum}}{d_{atm}} \; x \; 100 \quad (1)$$

$$\text{Bifilm Index} = \sum \; (Pore \; Lenght) \quad (2)$$

$$\text{Fluidity Index} = \frac{Liquid \; metal \; feed \; distance \; (mm)}{Cross \; section \; thickness \; (mm)} \quad (3)$$

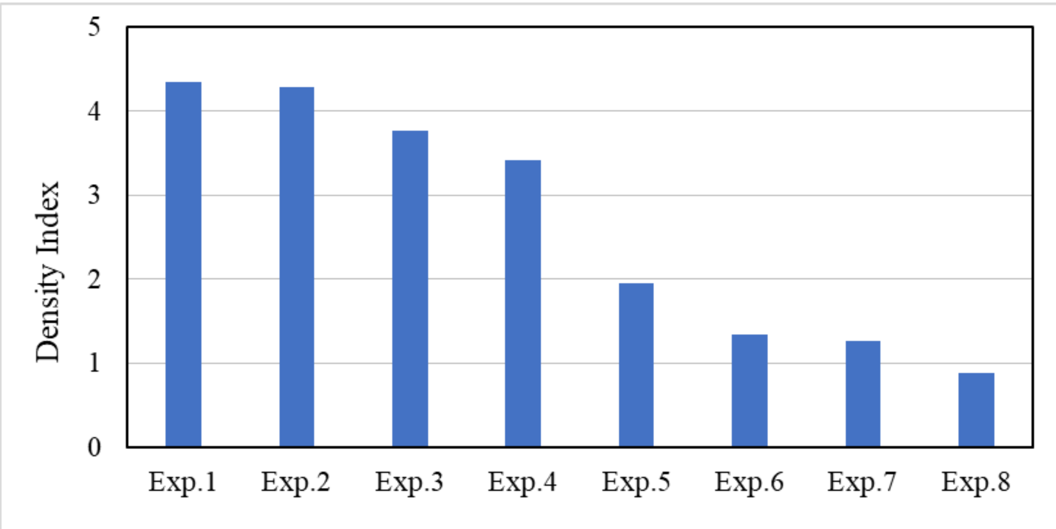

Fig. 2. Average density index values of the RPT samples

As shown in Figure 2, noticeable differences were observed in the average density index values of the samples. Depending on the applied rotary degassing parameters, the density index varied between 0.89 and 4.35. The highest density index value (4.35) was measured in Experiment 1, while the lowest (0.89) was recorded in Experiment 8. The lowest value corresponded to the condition with a higher gas flow rate. Following the density measurements, the RPT samples were sectioned, ground, and scanned to obtain digital images of the internal porosity. A sharp decrease in density index was observed when the rotor speed increased from 200 to 500 rpm, indicating a significant improvement in melt cleanliness. Increasing degassing time and gas flow rate provided additional but secondary reductions in density index. Representative scanned sample images are shown in Figure 3, and the average bifilm index values obtained from all experiments are presented in Figure 4.

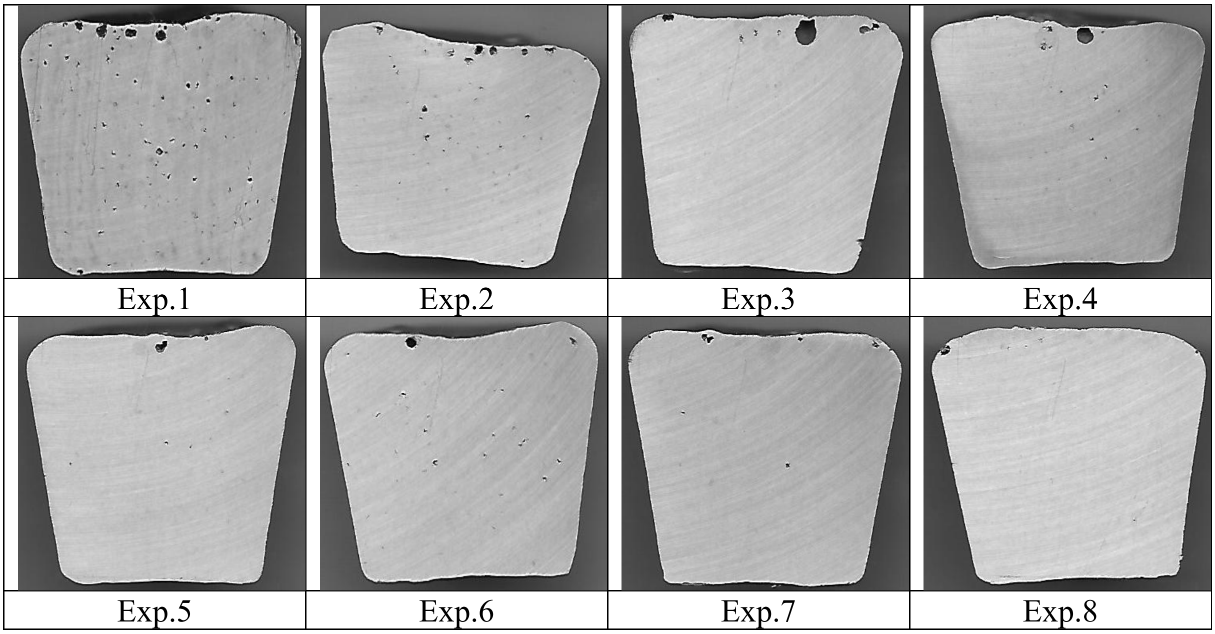

Fig. 3. Sectional surface images of the RPT samples

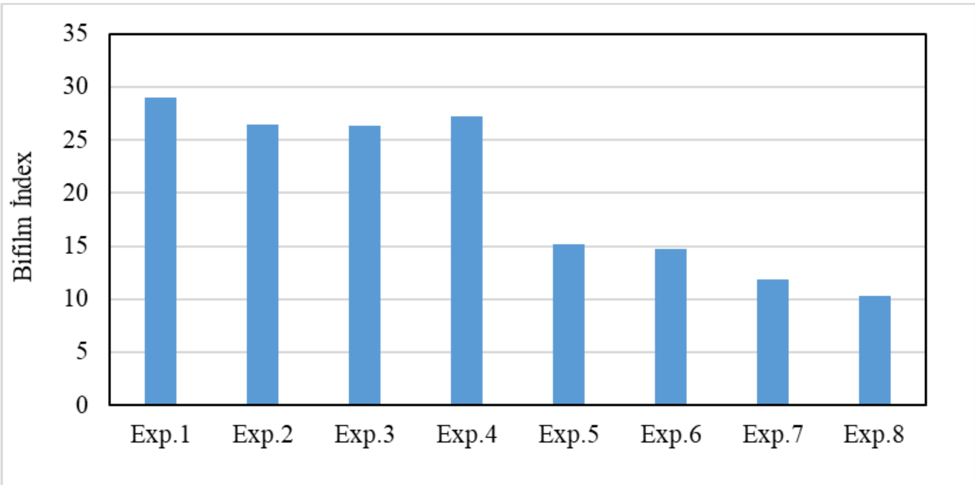

Fig. 4. Bifilm index graph of the RPT samples

As shown in Figure 4, the average bifilm index values indicate that the highest value (29) was obtained in Experiment 1. In general, the results reveal that rotor speed is a dominant parameter influencing melt cleanliness. When the rotor speed increased from 200 rpm to 500 rpm, the melt cleanliness improved significantly, leading to a noticeable reduction in the density index values. Ni et al. [19] reported that rotary impeller degassing in scrap-based A356 alloys enhances microstructural homogeneity and results in finer and more uniformly distributed eutectic Si particles. In agreement with their findings, the present study revealed that increasing rotor speed during the degassing process effectively reduced inclusion content, improved microstructural integrity, and led to a significant decrease in the bifilm index. Furthermore, Rathinasuriyan et al. [20] stated that the distribution characteristics of gas bubbles in rotary impeller degassing systems directly affect the cleaning efficiency. This observation is consistent with our results, where higher rotor speed promoted a more uniform dispersion of gas bubbles within the melt, enhancing the gas–metal interaction surface and consequently reducing the density index values.

3.3. Fluidity Test Results

In the casting of A356 aluminum alloy, the influence of parameters such as rotor speed, rotation time, and gas flow rate, which affect the fluidity behavior, was investigated using specimens obtained from the eight-channel fluidity mold. The representative images of the fluidity test samples are shown in Figure 5.

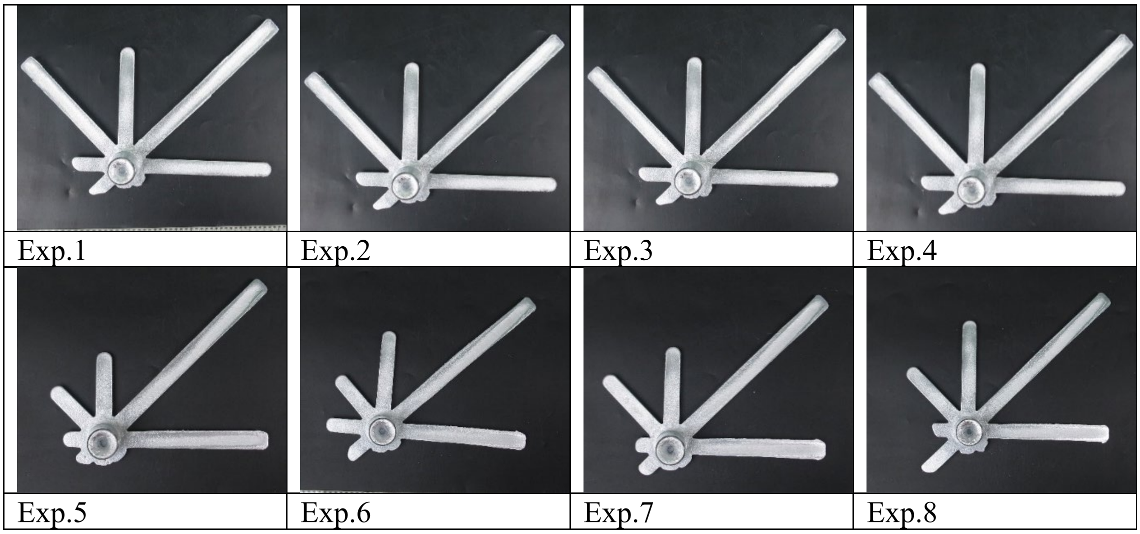

Fig. 5. Representative images of the eight-channel fluidity test samples

As shown in Figure 5, the fluidity test specimens revealed notable variations in the melt flow lengths under different experimental conditions. The melt flow distances were measured, and the corresponding fluidity index values were calculated. The measured melt flow lengths are presented in Table 3, while the calculated fluidity index values are illustrated in Figure 6.

Table 3.
Measured melt flow lengths of the experimental samples

	Liquid Metal Advancement Distance (mm)								**Fluidity Index (FI)**
	0,5	**1**	**2**	**3**	**4**	**5**	**6**	**8**	
Exp.1	7	9	35	46	170	131	168	250	183.78
Exp.2	6	6	21	49	127	142	80	250	149.57
Exp.3	5	7	26	44	169	175	175	250	182.33
Exp.4	5	6	26	27	89	107	175	250	142.07
Exp.5	5	5	15	23	62	81	175	250	122.28
Exp.6	6	8	34	49	66	108	175	250	151.85
Exp.7	6	7	25	95	95	95	175	250	166.33
Exp.8	8	10	58	94	128	128	175	250	204.35

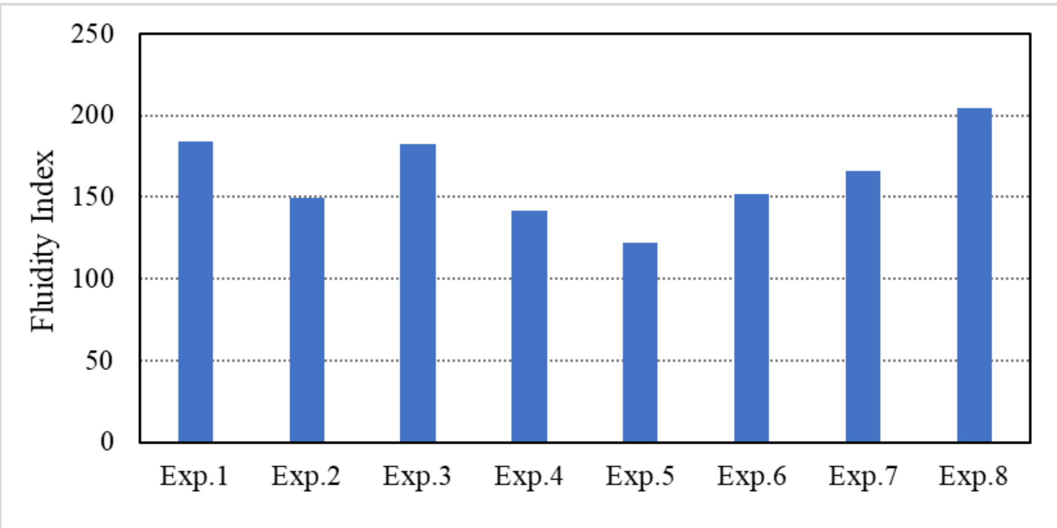

Fig. 6. Fluidity index graph of the experimental samples

Overall evaluation of Figure 6 indicates that the fluidity index increased with rising rotor speed and gas flow rate. The improvement in degassing efficiency at higher rotor speeds, along with the reduction of oxides and inclusions in the melt, enabled the molten metal to flow over a longer distance within the mold. Conversely, at lower rotor speeds and shorter rotation times, the inefficient removal of gases and inclusions led to a decrease in the fluidity index. The results indicate that improved melt cleanliness leads to enhanced fluidity behavior primarily at higher rotor speeds (500 rpm), where both bifilm index and fluidity show a consistent trend. At lower rotor speeds (200 rpm), fluctuations in fluidity suggest that melt cleanliness alone is insufficient without effective bubble dispersion.

Figure 7 illustrates the relationship between the bifilm index and the fluidity index obtained from the experimental conditions shown in Figures 4 and 6. A clear inverse correlation can be observed, where a reduction in bifilm index is accompanied by an increase in fluidity. This behaviour is consistent with the findings reported in the literature, which indicate that bifilms act as internal defects that disrupt melt continuity and hinder flow during solidification. Lower bifilm improves melt cleanliness, leading to enhanced feeding ability and smoother melt flow, which directly contributes to higher fluidity values. The sharp improvement in fluidity at lower bifilm indices suggests that melt cleanliness plays a more dominant role than thermal effects under the studied conditions. Similar trends have been reported for aluminium alloys subjected to effective degassing, where reduced bifilm content resulted in simultaneous improvements in fluidity and mechanical performance. Therefore, the present results confirm that optimisation of degassing parameters enhances melt quality primarily through the reduction of bifilm defects, which in turn improves fluidity behaviour [21].

The improvement in melt cleanliness observed in the present study can be directly attributed to the combined effects of rotary degassing parameters on hydrogen removal and bifilm reduction. According to the bifilm theory proposed by Campbell [1], oxide films entrained during melting and handling act as crack initiators and severely deteriorate melt quality. Rotary degassing enhances melt cleanliness primarily by promoting the flotation and separation of these bifilms through controlled gas bubble dispersion and melt agitation. Similar observations have been reported by Dispinar and Campbell [11], who demonstrated a strong correlation between bifilm content, porosity formation, and overall melt quality in aluminum alloys.

Among the investigated parameters, rotor speed was found to be the most influential factor affecting melt cleanliness. Increasing the rotor speed enhances the fragmentation of injected gas into finer bubbles, thereby increasing the gas–metal interfacial area and improving hydrogen diffusion kinetics. Rathinasuriyan et al. [20] reported that higher rotor speeds lead to a more homogeneous bubble size distribution, which significantly improves degassing efficiency and inclusion removal. The present findings are in good agreement with these results, as a substantial reduction in bifilm and density indices was achieved at 500 rpm compared to 200 rpm. Rotation time and gas flow rate played secondary but complementary roles in improving melt quality. Longer degassing durations allow sufficient time for hydrogen diffusion and bifilm flotation; however, excessive degassing may lead to re-oxidation and turbulence-induced bifilm formation [1]. Mostafaei et al. [23] similarly reported that while extended degassing time improves hydrogen removal, its effect becomes less significant compared to rotor speed once optimal bubble dispersion is achieved. Gas flow rate influences bubble population density, where higher flow rates promote increased bubble–melt interaction, but excessively high flow rates may result in bubble coalescence and reduced efficiency [24]. The optimal combination of rotor speed and gas flow rate observed in the present study confirms these competing mechanisms.

Overall, the enhancement of melt cleanliness is governed by the balance between effective bubble dispersion, controlled melt turbulence, and sufficient treatment duration. The reduction in bifilm index achieved under optimized degassing conditions directly reflects the suppression of oxide film entrainment and improved melt homogeneity. These mechanisms explain the observed improvements in fluidity and provide a sound physical basis for the subsequent enhancement of mechanical properties discussed in the following section. The consistency between the present results and the literature confirms that optimizing rotary degassing parameters is an effective strategy for achieving high melt quality in recycling-based A356 aluminum alloy production.

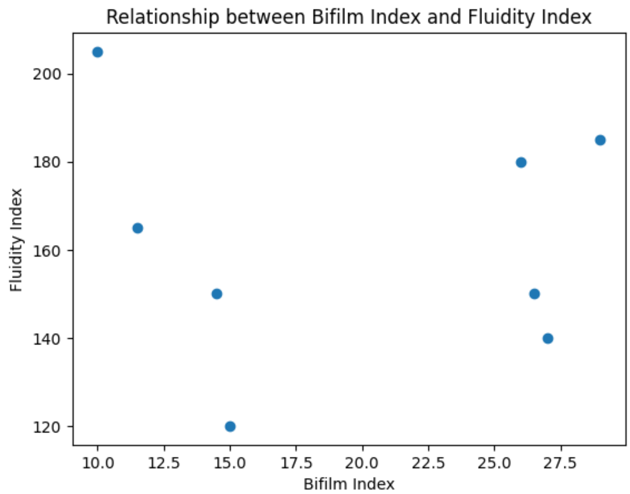

Fig. 7. Relationship between bifilm and fluidity

3.4. Mechanical Test Results

To determine the tensile strength, yield strength, and elongation (%) of the specimens, the samples obtained from the mechanical test mold were machined according to the standard tensile test geometry. The tensile tests were performed, and the average values of the obtained results were used to construct the graphs presented in Figure 8.

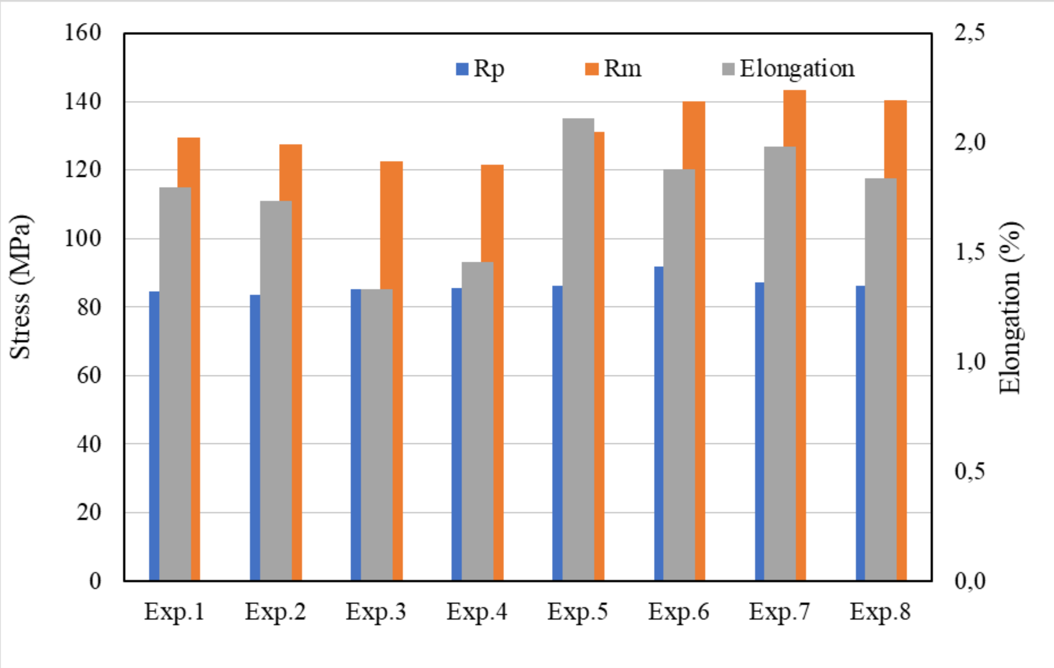

Fig. 8. Tensile test results of A356 aluminum alloy under different degassing parameters

As shown in Figure 8, the yield strength (Rp) ranged between 84 and 92 MPa, with the highest value obtained in Experiment 6 (91.77 MPa) and the lowest in Experiment 2 (83.95 MPa). The ultimate tensile strength (Rm) varied between 120 and 144 MPa, with the highest values (~140 MPa) recorded in Experiments 7 and 8. These improvements are primarily attributed to the enhanced efficiency of the rotary degassing process, which effectively reduced hydrogen and oxide inclusions in the melt. Increasing rotor speed improved melt homogenization and facilitated the flotation of inclusions to the surface, thereby reducing porosity. Consequently, the specimens from Experiments 7 and 8 exhibited higher strength and ductility, while those produced at lower rotor speeds (Experiments 3 and 4) showed premature fracture due to micro-porosity, resulting in lower tensile and elongation values.

The mechanical test results obtained in this study are largely consistent with previously reported findings. Lazaro-Nebreda et al. [22] demonstrated that improving degassing efficiency through high shear melt conditioning (HSMC) reduces porosity and enhances the mechanical strength of A356 alloy. Similarly, in the present study, increasing rotor speed led to improved melt cleanliness, resulting in a noticeable increase in tensile and yield strength values. Mostafaei et al. [23] systematically investigated the influence of degassing parameters and reported that optimizing both rotor speed and gas flow rate significantly reduced hydrogen content in the melt, thereby improving mechanical properties. Consistent with their observations, the present study also found that the combination of high gas flow rate (10 L/min) and rotor speed (500 rpm) yielded higher tensile and elongation values compared to lower-speed conditions. Moreover, Bogdanoff et al. [24] highlighted that rotary degassing of recycled Al–Si alloys not only improves melt quality but also reduces energy consumption, contributing to more sustainable casting practices. In this context, our results confirm that even at a high scrap ratio (80%), optimized degassing parameters can ensure both excellent melt cleanliness and mechanical performance. On the other hand, Gyarmati et al. [25] and Podaril et al. [26] showed that purging gas type (N_2/Ar) and rotor wear condition have significant effects on degassing efficiency and melt cleanliness. At 200 rpm, increasing degassing time and gas flow rate may promote melt turbulence, leading to bifilm re-entrainment and reduced mechanical performance. In contrast, at 500 rpm, effective bubble dispersion and controlled flow conditions improve bifilm flotation, resulting in enhanced tensile strength and elongation. Similar turbulence-related effects have been reported in the literature. These findings provide valuable guidance for future studies aimed at evaluating the influence of rotor material, design, and gas composition on mechanical performance and overall process optimization.

4. Conclusion

In this study, the effects of rotary degassing parameters—namely rotor speed, rotation time, and gas flow rate—on melt cleanliness were systematically investigated for A356 aluminum alloy containing 20% primary and 80% scrap material. The main findings are summarized as follows:

– Rotor speed was identified as the most critical parameter affecting melt cleanliness. Increasing the rotor speed from 200 rpm to 500 rpm significantly reduced both the density index and bifilm index, indicating a lower amount of gas and inclusions within the melt.
– Increasing the gas flow rate (10 L/min) showed limited improvement at lower rotor speeds, but when combined with higher speeds, it provided an additional enhancement in melt quality.

– Extending the rotation time to 10 minutes slightly improved cleanliness and mechanical performance compared to 5 minutes; however, from an economic perspective, rotation time was found to be less influential than rotor speed.
– RPT and bifilm analyses confirmed consistent trends, showing that increasing rotor speed resulted in a significant decrease in the density and bifilm indices, indicating improved melt cleanliness and reduced inclusion content.
– Fluidity tests revealed that the fluidity index increased under cleaner melt conditions, confirming that reduced oxide films and gas porosity enhance flow behavior.
– In terms of mechanical properties, the highest tensile strength values were obtained in Exp.7 and Exp.8, both conducted with high rotor speed and optimal gas flow. Minor improvements were also observed in elongation.

Overall, the combination of high rotor speed (500 rpm), optimal gas flow rate (10 L/min), and sufficient rotation time (10 min) achieved the best melt cleanliness and mechanical performance. These findings present an effective process optimization strategy for foundries operating with high scrap ratios in recycling-oriented production. The results are consistent with previously reported bifilm theory and degassing mechanisms, and they hold significant potential for direct industrial implementation in aluminum casting operations.

Acknowledgement

The authors would like to express their sincere gratitude to Cevher Jant Sanayii A.Ş. for their valuable support in the realization of this study. This research was conducted within the framework of the Poland–Turkey Bilateral Cooperation Project No. 122N144, supported by TÜBİTAK.

References

[1] Campbell, J. (2015). *Complete casting handbook: metal casting processes, metallurgy, techniques and design*. Butterworth-Heinemann.

[2] Kutsal, U., Colak, M. & Ertugrul, O. (2025). Relationship between aluminum liquid metal quality and defects. *International Journal of Metalcasting*. 20, 2080-2095. https://doi.org/10.1007/s40962-025-01733-1.

[3] Rooy, E.L. (1990). Introduction to aluminum and aluminum alloys. In ASM Handbook Committee (Eds.) *Properties and selection: nonferrous alloys and special-purpose materials* (pp. 3-14). ASM International.

[4] Chen, W.F., Lui, E.M. (2005). *Handbook of structural engineering*. CRC press.

[5] Padamata, S.K., Yasinskiy, A. & Polyakov, P. (2021). A review of secondary aluminum production and its byproducts. *The Journal of The Minerals, Metals & Materials Society (TMS)*. 73(9), 2603-2614. https://doi.org/10.1007/s11837-021-04802-y.

[6] Zhu, S., Gao, C., Song, K., Chen, M., Wu, F. & Li, X. (2022). An assessment of environmental impacts and economic benefits of multiple aluminum production methods. *Journal of Cleaner Production*. 370, 133523, 1-11. DOI: 10.1016/j.jclepro.2022.133523.

[7] Dispinar, D. (2006). *Determination of metal quality of aluminium and its alloys*. Doctoral dissertation, University of Birmingham.

[8] Durmuş, M., Dispinar, D., Gavgali, M., Uslu, E. & Çolak, M. (2025). Evaluation of Fe content on the fluidity of A356 aluminum alloy by new fluidity index. *International Journal of Metalcasting*. 19(3), 1590-1604. https://doi.org/10.1007/s40962-024-01396-4.

[9] Kaufman, J.G., Rooy, E.L. (2004). *Aluminum alloy castings: properties, processes, and applications*. ASM International.

[10] Chiesa, F., Regimbal, P. (2001). Distinguishing microporosity from macroshrinkage when modeling solidification of A 356 castings. In *Transactions of the American Foundry Society and the One Hundred Fifth Annual Castings Congress* (pp. 1-11).

[11] Dispinar, D. & Campbell, J. (2011). Porosity, hydrogen and bifilm content in Al alloy castings. *Materials Science and Engineering: A*. 528(10-11), 3860-3865. https://doi.org/10.1016/j.msea.2011.01.084.

[12] Yüksel, Ç., Aybarc, U., Erzi, E., Dispinar, D., Cigdem, M. (2019, February). Melt cleaning efficiency of various fluxes for A356 alloy. In *Shape Casting: 7th International Symposium Celebrating Prof. John Campbell's 80th Birthday* (pp. 273-280). Cham: Springer International Publishing.

[13] Hudson, S.W. & Apelian, D. (2016). Inclusion detection in molten aluminum: current art and new avenues for in situ analysis. *International Journal of Metalcasting*. 10(3), 289-305. https://doi.org/10.1007/s40962-016-0030-x.

[14] Uslu, E., Dağ, M.M. & Çolak, M. (2023). Design and manufacturing of reduced pressure test machine for determination of liquid aluminum quality in casting. *Turkish Journal of Electromechanics and Energy*. 8(3), 85-89.

[15] Vijayan, V., Shetty, A., Hiremath, S., Kumar, P. & HM, V. (2023). A comprehensive analysis of cooling curves, fluidity, inclusions, porosity, and microstructure of NaCl-KCl-NaF flux treated Al-12Si alloy. *Materials Research Express*. 10(12), 126506, 1-12. DOI: 10.1088/2053-1591/ad135b.

[16] Djurdjević, M.B., Odanović, Z. & Pavlović-Krstić, J. (2010). Melt quality control at aluminum casting plants. *Metallurgical & Materials Engineering*. 16(1), 63-76.

[17] Tigli, A., Tokatli, M., Uslu, E., Colak, M. & Dispinar, D. (2023). Correlation between K-value, density index and bifilm index in determination of liquid Al cleanliness. *Archives of Foundry Engineering*. 23(3), 22-29. DOI: 10.24425/afe.2023.144311.

[18] Brůna, M. & Sládek, A. (2011). Hydrogen analysis and effect of filtration on final quality of castings from aluminium alloy AlSi7Mg0, 3. *Archives of Foundry Engineering*. 11(1), 5-10.

[19] Ni, H., Sun, B., Jiang, H. & Ding, W. (2003). Effects of rotating impeller degassing on microstructure and mechanical properties of the A356 scraps. *Materials Science and Engineering: A*. 352(1-2), 294-299. ISSN (1897-3310).

[20] Rathinasuriyan, C., Karthik, K. & Sridhar, K. (2023). Investigation of degassing on aluminum alloy by rotatory impeller degasser. *Materials Today: Proceedings.* DOI: 10.1016/j.matpr.2023.03.263.

[21] Di Sabatino, M., Arnberg, L., Rørvik, S. & Prestmo, A. (2005). The influence of oxide inclusions on the fluidity of Al–7 wt.%Si alloy. *Materials Science and Engineering: A*. 413-414, 272-276. https://doi.org/10.1016/j.msea.2005.08.175.
[22] Lazaro-Nebreda, J., Patel, J.B. & Fan, Z. (2021). Improved degassing efficiency and mechanical properties of A356 aluminium alloy castings by high shear melt conditioning (HSMC) technology. *Journal of Materials Processing Technology*. 294, 117146, 1-12. DOI: 10.1016/j.jmatprotec.2021.117146.
[23] Mostafaei, M., Ghobadi, M., Eisaabadi B, G., Uludağ, M. & Tiryakioğlu, M. (2016). Evaluation of the effects of rotary degassing process variables on the quality of A357 aluminum alloy castings. *Metallurgical and Materials Transactions B*. 47(6), 3469-3475. https://doi.org/10.1007/s11663-016-0786-7.
[24] Bogdanoff, T., Tiryakioğlu, M., Liljenfors, T., Jarfors, A.E., Seifeddine, S. & Ghassemali, E. (2023). On the effectiveness of rotary degassing of recycled Al-Si alloy melts: The effect on melt quality and energy consumption for melt preparation. *Sustainability*. 15(6), 5189, 1-10. https://doi.org/10.3390/su15065189.
[25] Gyarmati, G., Vincze, F., Fegyverneki, G., Kéri, Z., Mende, T. & Molnár, D. (2022). The effect of rotary degassing treatments with different purging gases on the double oxide- and nitride film content of liquid aluminum alloys. *Metallurgical and Materials Transactions B*. 53(2), 1244-1257. https://doi.org/10.1007/s11663-021-02414-0.
[26] Podaril, M., Prášil, T., Majernik, J., Kampf, R., Socha, L., Gryc, K. & Gráf, M. (2022). Aluminum melt degassing process evaluation depending on the design and the degree of the FDU unit graphite rotor wear. *Materials*. 15(14), 4924, 1-15. https://doi.org/10.3390/ma15144924.